

New estimation methodology of six complex aerodynamic admittance functions

Y. Han^{1,2}, Z.Q. Chen^{1*} and X.G. Hua¹

¹Wind Engineering Research Center, College of Civil Engineering, Hunan University, Changsha 410082, Hunan, P. R. China

²School of Civil Engineering and Architecture, Changsha University of Science & Technology, Changsha 410076, Hunan, P. R. China

(Received January 7, 2009, Accepted February 3, 2010)

Abstract. This paper describes a new method for the estimation of six complex aerodynamic admittance functions. The aerodynamic admittance functions relate buffeting forces to the incoming wind turbulent components, of which the estimation accuracy affects the prediction accuracy of the buffeting response of long-span bridges. There should be two aerodynamic admittance functions corresponding to the longitudinal and vertical turbulent components, respectively, for each gust buffeting force. Therefore, there are six aerodynamic admittance functions in all for the three buffeting forces. Sears function is a complex theoretical expression for the aerodynamic admittance function for a thin airfoil. Similarly, the aerodynamic admittance functions for a bridge deck should also be complex functions. This paper presents a separated frequency-by-frequency method for estimating the six complex aerodynamic admittance functions. A new experimental methodology using an active turbulence generator is developed to measure simultaneously all the six complex aerodynamic admittance functions. Wind tunnel tests of a thin plate model and a streamlined bridge section model are conducted in turbulent flow. The six complex aerodynamic admittance functions, determined by the developed methodology are compared with the Sears functions and Davenport's formula.

Keywords: admittance functions; Sears function; thin plates; buffeting forces; long-span bridges.

1. Introduction

The advancements in modeling of the buffeting forces are generally accompanied by the developments of the aerodynamic admittance functions that relate buffeting forces to the incoming wind turbulent components. The accuracy of predicting buffeting response of a long-span bridge depends largely on the accurate estimations of the aerodynamic admittance functions. Sears function, which is a theoretical expression for the aerodynamic admittance function for an idealized thin airfoil, is conventionally applied to the gust response analysis of long-span bridges (Mendes and Branco 2001, Denoel and Degee 2006). Thin airfoil dynamic force theories depend on unique circulation functions (Theodorsen 1935, Sears 1941, Liepmann 1952). However, the circulation functions cannot be realized for bluff bodies that experience flow separation. Extending the theoretical thin-airfoil force coefficients to the bluff bodies presented by bridge deck sections is

* Corresponding Author, Professor, E-mail: zqchen@hnu.cn

basically incorrect from both mathematical and physical viewpoints. The common use of the Sears function in the context of bridge deck buffeting can be viewed only as a suggested approximation. Davenport (1962) also derived a formula for aerodynamic admittance function of drag force in relation to horizontal turbulence component.

Since the thin airfoil theory does not apply to bluff bodies, aerodynamic admittance functions of bridge deck sections cannot be defined analytically. They are usually determined experimentally by wind tunnel tests or derived from flutter derivatives as proposed by Scanlan and other researchers (Scanlan 1993, Scanlan and Jones 1999, Scanlan 2000, Chen and Kareem 2002, Tubino 2005) and the relationships are verified by Hatanaka and Tanaka (2002, 2008). Jancauskas and Melbourne (1986) and Kawatani and Kim (1992) studied the aerodynamic admittance functions for rectangular sections by experiments and found that they are different from Sears function. An experimental comparison of the aerodynamic admittance functions for a thin plate and different streamlined bridge decks was performed by Larose and Livesey (1997). Larose and Mann (1998) analytically obtained the aerodynamic admittance functions for a thin airfoil considering two wave-numbers and compared the analytical results with experimental ones obtained for a family of streamlined deck sections. Zhou and Kareem (2003) developed a procedure that uses high frequency base balance to estimate aerodynamic admittance functions and noted some discrepancies between experimentally obtained and theoretical aerodynamic admittance functions in the high frequency range.

The methods used in the literature reviewed above are usually direct estimation methods which mean the modul square of aerodynamic admittance function is estimated by the ratio of the power spectral density functions of fluctuating forces and the wind velocity fluctuations. However, since the aerodynamic admittance functions for a bridge deck are complex functions like Sears function (Sears 1941), they cannot be obtained by this approach. Diana, *et al.* (2002, 2004) developed the concept of complex aerodynamic admittance functions and identified three complex aerodynamic admittance functions for realistic bridge sections associated with vertical gusts by using an active turbulence generator. However, there are six aerodynamic admittance functions for gust forces corresponding to the longitudinal and vertical turbulent components. This paper presents a separated frequency-by-frequency methodology for estimating the six complex aerodynamic admittance functions using an active turbulence generator (Han 2007). The six complex aerodynamic admittance functions for a thin plate were identified by using the developed methodology and compared with Sears function and Davenport's formulae.

2. Theoretical basis of the new estimation methodology

The aerodynamic lift force, drag force, and pitching moment of a bridge deck with a length of D can be defined as (Chen and Kareem 2002)

$$L_b(t) = \frac{1}{2}\rho U^2 BD \left[2C_L \chi_{Lu} \frac{u(t)}{U} + (C'_L + C_D) \chi_{Lw} \frac{w(t)}{U} \right] \quad (1a)$$

$$D_b(t) = \frac{1}{2}\rho U^2 BD \left[2C_D \chi_{Du} \frac{u(t)}{U} + (C'_D - C_L) \chi_{Dw} \frac{w(t)}{U} \right] \quad (1b)$$

$$M_b(t) = \frac{1}{2}\rho U^2 B^2 D \left[2C_M \chi_{Mu} \frac{u(t)}{U} + C'_M \chi_{Mw} \frac{w(t)}{U} \right] \quad (1c)$$

where ρ is the air density; B is the deck width; U is the mean longitudinal wind velocity; $u(t)$ and $w(t)$ are the longitudinal and vertical turbulence wind components, respectively; C_D, C_L, C_M are the drag force, lift force, and pitching moment coefficients, respectively; C'_D, C'_L, C'_M are the derivatives of C_D, C_L and C_M with respect to wind attack angle, respectively; and χ_{Rk} ($R = L, D, M; k = u, w$) are aerodynamic admittance functions.

To explain the concept, suppose that $u(t)$ and $w(t)$ are time-varying harmonic turbulent wind components expressed as:

$$u(t) = A \cos(\omega_1 t + \varphi_1) = A \cos(2\pi k_1 t / T + \varphi_1) \quad (2a)$$

$$w(t) = B \cos(\omega_2 t + \varphi_2) = B \cos(2\pi k_2 t / T + \varphi_2) \quad (2b)$$

where A and B are the amplitude of harmonic functions $u(t)$ and $w(t)$, respectively; ω_1 and ω_2 are vibration circular frequency of $u(t)$ and $w(t)$, respectively, and $\omega_1 \neq \omega_2$; T is the total duration and $T = 2\pi k_1 / \omega_1 = 2\pi k_2 / \omega_2$; k_1 and k_2 are random positive whole numbers corresponding to ω_1 and ω_2 ; and φ_1 and φ_2 are initial phase angle of $u(t)$ and $w(t)$, respectively.

By using Fast Fourier Transform (FFT) algorithm, Eqs. (2a-2b) are transformed as:

$$F[L_b(t)] = \frac{1}{2} \rho U^2 B D \left[2 C_L \chi_{Lu} \frac{F[u(t)]}{U} + (C'_L + C_D) \chi_{Lw} \frac{F[w(t)]}{U} \right] \quad (3a)$$

$$F[D_b(t)] = \frac{1}{2} \rho U^2 B D \left[2 C_D \chi_{Du} \frac{F[u(t)]}{U} + (C'_D - C_L) \chi_{Dw} \frac{F[w(t)]}{U} \right] \quad (3b)$$

$$F[M_b(t)] = \frac{1}{2} \rho U^2 B^2 D \left[2 C_M \chi_{Mu} \frac{F[u(t)]}{U} + C'_M \chi_{Mw} \frac{F[w(t)]}{U} \right] \quad (3c)$$

where the sign $F[]$ denotes the operation of FFT algorithm.

The FFTs of $u(t)$ and $w(t)$ are expressed as:

$$\begin{aligned} F[u(t)] &= \int_{-T/2}^{T/2} u(t) e^{-i\omega t} dt = \int_{-T/2}^{T/2} A \cos(2\pi k_1 t / T + \varphi_1) e^{-i(2\pi k t / T)} dt \\ &= \frac{AT}{2} e^{i\varphi_1} \frac{\sin \pi(k_1 - k)}{\pi(k_1 - k)} + \frac{AT}{2} e^{-i\varphi_1} \frac{\sin \pi(k_1 + k)}{\pi(k_1 + k)} \\ &= \frac{AT}{2} e^{i\varphi_1} \Theta(\omega_1 - \omega) + \frac{AT}{2} e^{-i\varphi_1} \Theta(\omega_1 + \omega) \end{aligned} \quad (4a)$$

$$\begin{aligned} F[w(t)] &= \int_{-T/2}^{T/2} w(t) e^{-i\omega t} dt = \int_{-T/2}^{T/2} B \cos(2\pi k_2 t / T + \varphi_2) e^{-i(2\pi k t / T)} dt \\ &= \frac{BT}{2} e^{i\varphi_2} \frac{\sin \pi(k_2 - k)}{\pi(k_2 - k)} + \frac{BT}{2} e^{-i\varphi_2} \frac{\sin \pi(k_2 + k)}{\pi(k_2 + k)} \\ &= \frac{BT}{2} e^{i\varphi_2} \Theta(\omega_2 - \omega) + \frac{BT}{2} e^{-i\varphi_2} \Theta(\omega_2 + \omega) \end{aligned} \quad (4b)$$

where

$$\Theta(\omega_1 - \omega) = \frac{\sin(\omega_1 - \omega)T/2}{(\omega_1 - \omega)T/2}, \quad \Theta(\omega_1 + \omega) = \frac{\sin(\omega_1 + \omega)T/2}{(\omega_1 + \omega)T/2} \quad (5a)$$

$$\Theta(\omega_2 - \omega) = \frac{\sin(\omega_2 - \omega)T/2}{(\omega_2 - \omega)T/2}, \quad \Theta(\omega_2 + \omega) = \frac{\sin(\omega_2 + \omega)T/2}{(\omega_2 + \omega)T/2} \quad (5b)$$

Suppose that the FFTs of $L_b(t)$, $D_b(t)$ and $M_b(t)$ are defined as:

$$F[L_b(t)] = L_b(\omega) \quad (6a)$$

$$F[D_b(t)] = D_b(\omega) \quad (6b)$$

$$F[M_b(t)] = M_b(\omega) \quad (6c)$$

Replacing Eqs. (4a-4b) and (6a-6c) into Eq. (3) provides:

$$\begin{aligned} L_b(\omega) = & \frac{1}{2}\rho U^2 BDC_L \frac{2}{U} \chi_{Lu} \frac{AT}{2} (e^{i\varphi_1} \Theta(\omega_1 - \omega) + e^{-i\varphi_1} \Theta(\omega_1 + \omega)) \\ & + \frac{1}{2}\rho U^2 BD \frac{(C'_L - C_D)}{U} \chi_{Lw} \frac{BT}{2} (e^{i\varphi_2} \Theta(\omega_2 - \omega) + e^{-i\varphi_2} \Theta(\omega_2 + \omega)) \end{aligned} \quad (7a)$$

$$\begin{aligned} D_b(\omega) = & \frac{1}{2}\rho U^2 BDC_D \frac{2}{U} \chi_{Du} \frac{AT}{2} (e^{i\varphi_1} \Theta(\omega_1 - \omega) + e^{-i\varphi_1} \Theta(\omega_1 + \omega)) \\ & + \frac{1}{2}\rho U^2 BD \frac{(C'_D - C_L)}{U} \chi_{Dw} \frac{BT}{2} (e^{i\varphi_2} \Theta(\omega_2 - \omega) + e^{-i\varphi_2} \Theta(\omega_2 + \omega)) \end{aligned} \quad (7b)$$

$$\begin{aligned} M_b(\omega) = & \frac{1}{2}\rho U^2 BDC_M \frac{2}{U} \chi_{Mu} \frac{AT}{2} (e^{i\varphi_1} \Theta(\omega_1 - \omega) + e^{-i\varphi_1} \Theta(\omega_1 + \omega)) \\ & + \frac{1}{2}\rho U^2 B^2 D \frac{C'_M}{U} \chi_{Mw} \frac{BT}{2} (e^{i\varphi_2} \Theta(\omega_2 - \omega) + e^{-i\varphi_2} \Theta(\omega_2 + \omega)) \end{aligned} \quad (7c)$$

If $\omega = \omega_1$, Eqs. (7a-7c) turn into:

$$L_b(\omega_1) = \frac{1}{2}\rho U^2 BDC_L \frac{2}{U} \chi_{Lu} \cdot \frac{AT}{2} e^{i\varphi_1} \quad (8a)$$

$$D_b(\omega_1) = \frac{1}{2}\rho U^2 BDC_D \frac{2}{U} \chi_{Du} \cdot \frac{AT}{2} e^{i\varphi_1} \quad (8b)$$

$$M_b(\omega_1) = \frac{1}{2}\rho U^2 B^2 DC_M \frac{2}{U} \chi_{Mu} \cdot \frac{AT}{2} e^{i\varphi_1} \quad (8c)$$

According to Eq. (8), the complex aerodynamic admittance functions χ_{Lu} , χ_{Du} and χ_{Mu} corresponding to longitudinal turbulent component $u(t)$ can be easily derived as:

$$\chi_{Lu}(\omega_1) = \frac{L_b(\omega_1)}{\frac{1}{2}\rho U^2 B D C_L \frac{2}{U} \cdot \frac{BT}{2} e^{i\varphi_1}} \quad (9a)$$

$$\chi_{Du}(\omega_1) = \frac{D_b(\omega_1)}{\frac{1}{2}\rho U^2 B D C_D \frac{2}{U} \cdot \frac{BT}{2} e^{i\varphi_1}} \quad (9b)$$

$$\chi_{Mu}(\omega_1) = \frac{M_b(\omega_1)}{\frac{1}{2}\rho U^2 B^2 D C_M \frac{2}{U} \cdot \frac{BT}{2} e^{i\varphi_1}} \quad (9c)$$

If $\omega = \omega_2$, Eqs. (7a-7c) turn into:

$$L_b(\omega_2) = \frac{1}{2}\rho U^2 B D \frac{(C_L + C_D)}{U} \chi_{Lw} \cdot \frac{BT}{2} e^{i\varphi_2} \quad (10a)$$

$$D_b(\omega_2) = \frac{1}{2}\rho U^2 B D \frac{(C_D - C_L)}{U} \chi_{Dw} \cdot \frac{BT}{2} e^{i\varphi_2} \quad (10b)$$

$$M_b(\omega_2) = \frac{1}{2}\rho U^2 B^2 D \frac{C_M}{U} \chi_{Mw} \cdot \frac{BT}{2} e^{i\varphi_2} \quad (10c)$$

From Eq. (10), the complex aerodynamic admittance functions χ_{Lw} , χ_{Dw} and χ_{Mw} corresponding to the vertical turbulent component $w(t)$ can be easily derived as:

$$\chi_{Lw}(\omega_2) = \frac{L_b(\omega_2)}{\frac{1}{2}\rho U^2 B D \frac{(C_L + C_D)}{U} \cdot \frac{BT}{2} e^{i\varphi_2}} \quad (11a)$$

$$\chi_{Dw}(\omega_2) = \frac{D_b(\omega_2)}{\frac{1}{2}\rho U^2 B D \frac{(C_D - C_L)}{U} \cdot \frac{BT}{2} e^{i\varphi_2}} \quad (11b)$$

$$\chi_{Mw}(\omega_2) = \frac{M_b(\omega_2)}{\frac{1}{2}\rho U^2 B^2 D \frac{C_M}{U} \cdot \frac{BT}{2} e^{i\varphi_2}} \quad (11c)$$

Up to now, the complex formulations of the six aerodynamic admittance functions are given as Eqs. (9) and (11). If there is a special experimental setup which can generate the harmonic oscillating longitudinal and vertical velocity components with different frequencies simultaneously, the six complex aerodynamic admittance functions can be estimated at one time, frequency-by-frequency.

3. Experimental technique

An active turbulence generator is developed for generating simultaneously the harmonic oscillating longitudinal and vertical wind velocity components with different frequencies in the HD-

2 wind tunnel at Hunan University. The experimental set-up as shown in Fig. 1 is made of a series of wings linked together to produce the harmonic oscillating vertical wind velocity component and a series of motionless thin plates installed in the middle of wings to produce the harmonic oscillating longitudinal velocity component. The motions of all the wings are controlled by an AC servomotors and the motion frequency is controllable and does not depend on the mean wind velocity.

A number of tests are conducted to check the correlation between two points around the model in the wind field. The locations of measurement points cover the whole length and width of the sectional model, and are shown in Fig. 2. Two cobra probes are used to simultaneously measure the longitudinal/vertical turbulence components at two points as given in Fig. 2. Correlation coefficients are larger than 0.99 for both vertical and horizontal components for all the testing conditions; the incoming flow can be thus considered as a perfect 2D flow.

A force-measurement system as shown in Fig. 3 is set up and a five-component force balances at each support are used to measure the five-direction forces, allowing a calculation of the total drag force, lift force, and pitching moment. Because one side of the force-measurement equipment is set inside the wind tunnel, a fairings is designed to avoid the disturbance around the side of the force-measurement equipment inside the wind tunnel. By using the measured aerodynamic forces and the measured turbulence components, the six complex aerodynamic admittance functions, relating the

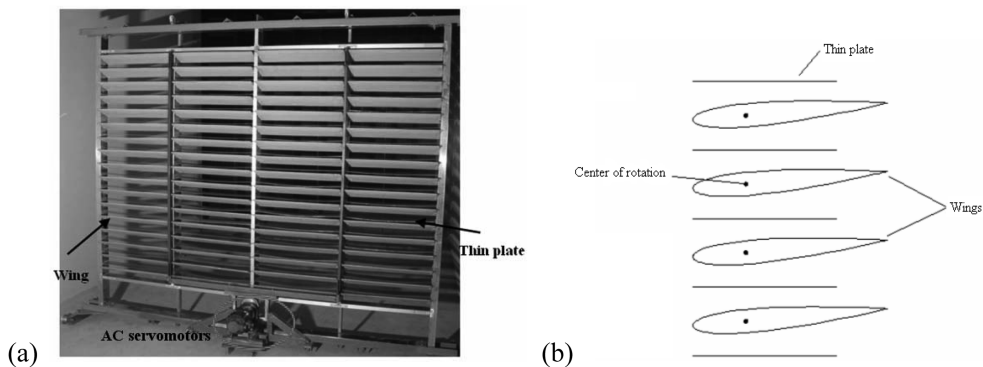


Fig. 1 An active turbulence generator: (a) actual deployment, (b) sketch

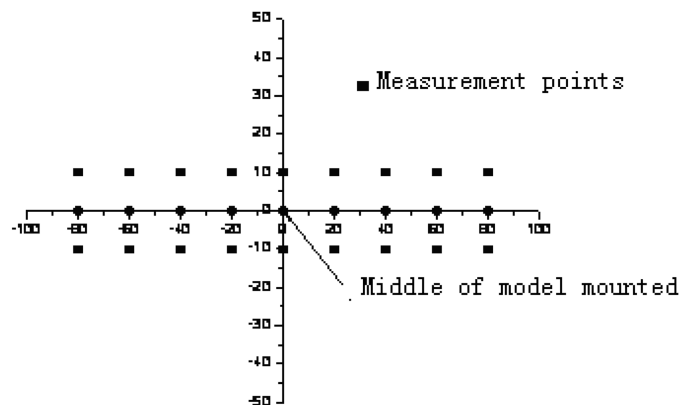


Fig. 2 Locations of measurement points of wind velocity (units: cm)

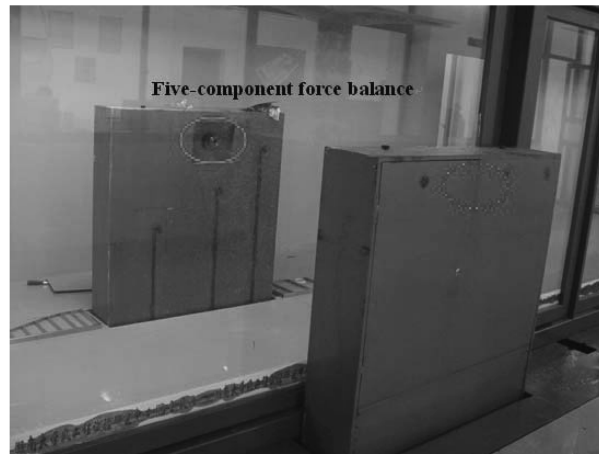


Fig. 3 The force-measurement equipment (with the left side inside the wind tunnel)

three buffeting forces to the two turbulent wind components, are then identified using Eqs. (9) and (11) by sweeping the mean wind velocity but keeping the vibration frequency of wings unchanged. It should be noted that the active turbulence generator developed by Diana, *et al.* (2002, 2004) can only produce the vertical turbulent wind component and therefore restricts itself to identification of the three aerodynamic admittance functions related to turbulent wind component w .

4. Turbulence flow characterization

Examples of experimentally generated time histories of turbulence components, obtained by driving the generator with a frequency of 1 Hz, are shown in Fig. 4. The mean horizontal wind speed is, for this test, 8 m/s. Fig. 5 shows the amplitude spectra of the longitudinal and vertical

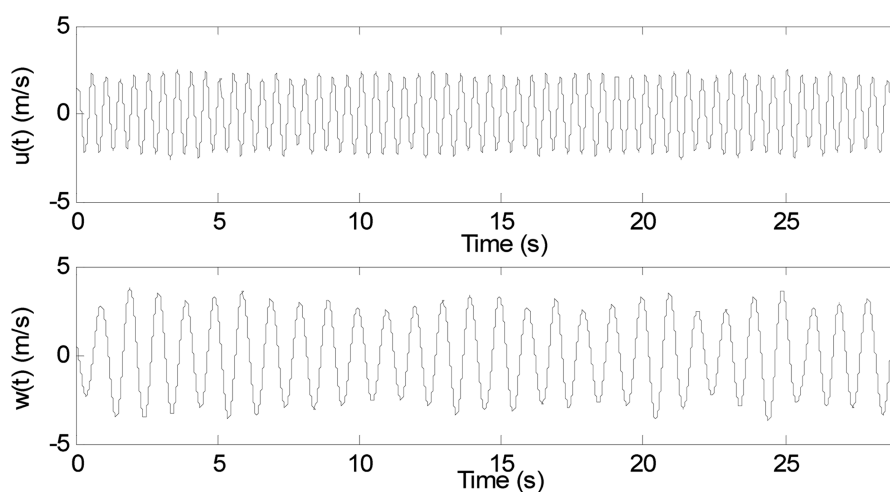


Fig. 4 The longitudinal and vertical turbulent components time histories

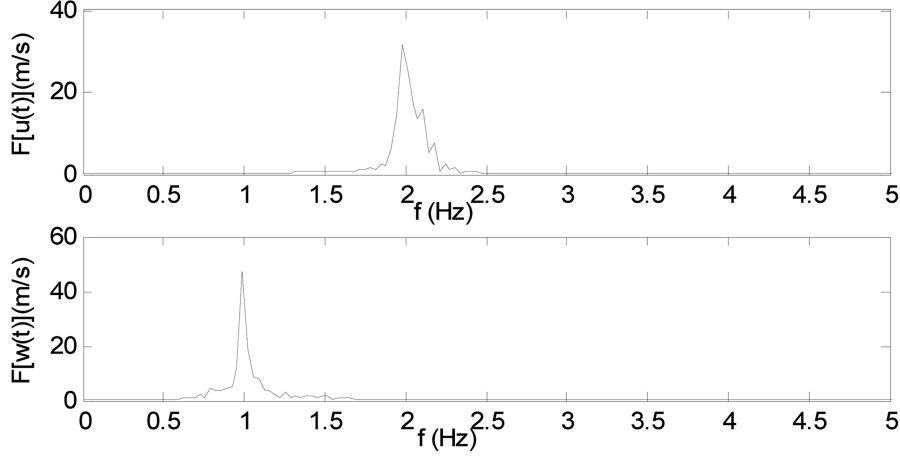


Fig. 5 The amplitude spectra of the longitudinal and vertical turbulent components

turbulent components. From Figs. 4 and 5, it is observed that the two turbulence components are mainly made up of just one harmonic component and the frequency of the vertical component is different from the frequency of the longitudinal one, as desired. They also show that the frequency of the vertical turbulence is identical with the frequency of the wings (1 Hz) and the frequency of the longitudinal turbulence (2 Hz) is twice the frequency of the wings.

5. Determination of complex aerodynamic admittance functions

As discussed earlier, the experimental procedure to obtain the complex aerodynamic admittance functions is based on the use of the developed active generator. Suppose that the generated turbulences have a vertical frequency ω_w and horizontal one ω_u . Similar to Eqs. (9) and (11), the six complex admittance functions can be obtained for the aerodynamic drag, lift and moment as:

$$\chi_{Lu}(\omega_u) = \frac{F[L(t)]}{\frac{1}{2}\rho U^2 B D C_L \frac{2}{U} \cdot F[u(t)]} \quad (12a)$$

$$\chi_{Du}(\omega_u) = \frac{F[D(t)]}{\frac{1}{2}\rho U^2 B D C_D \frac{2}{U} \cdot F[u(t)]} \quad (12b)$$

$$\chi_{Mu}(\omega_u) = \frac{F[M(t)]}{\frac{1}{2}\rho U^2 B^2 D C_M \frac{2}{U} \cdot F[u(t)]} \quad (12c)$$

$$\chi_{Lw}(\omega_w) = \frac{F[L(t)]}{\frac{1}{2}\rho U^2 B D \frac{(C_L + C_D)}{U} \cdot F[w(t)]} \quad (13a)$$

$$\chi_{Dw}(\omega_w) = \frac{F[D(t)]}{\frac{1}{2}\rho U^2 B D \frac{(C_D - C_L)}{U} \cdot F[w(t)]} \quad (13b)$$

$$\chi_{Mw}(\omega_w) = \frac{F[M(t)]}{\frac{1}{2}\rho U^2 B^2 D \frac{C_M}{U} \cdot F[w(t)]} \quad (13c)$$

where $\omega_u = 2\omega_w$.

Wind tunnel tests of a thin plate model and a streamlined bridge section model (as shown in Fig. 6) are conducted in turbulent flow. The thin plate section (length \times width \times depth = 155 cm \times 45 cm \times 2 cm) is made of ABS plates and there is an aluminum bar inside to improve the stiffness of the model. The streamlined section model is made of wood plates and there also is an aluminum bar inside. The section models are fixed on the force-measurement equipment firmly (as shown in Fig. 7) and the natural frequencies of the whole experimental system which is composed of the section model and the equipment are listed in Table 1. From Table 1, it is observed that the natural frequencies of the whole experimental equipment system are large enough to satisfy the need of stiffness.

Before identifying the aerodynamic admittance functions, the static aerodynamic coefficients of the sections must be measured. Figs. 8 and 9 show the drag force, lift force, and pitching moment coefficients of the thin plate section model and the streamlined section model, respectively. In this

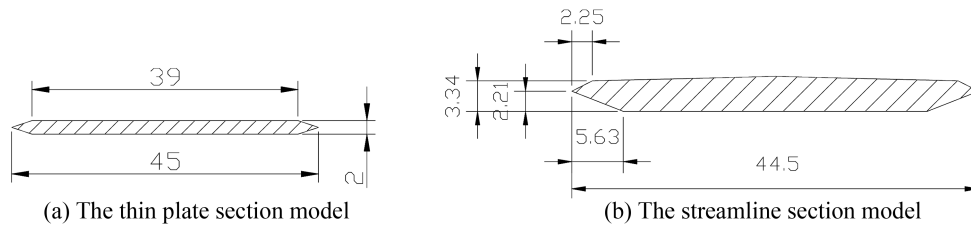


Fig. 6 The section models (unit. cm)



Fig. 7 The thin plate section model in the wind tunnel

Table 1 Frequencies of the whole experimental system

Motion direction	Frequencies (Hz)	
	The thin plate section model case	The streamlined section model case
Vertical bending	21.2	36.4
Lateral bending	45.6	58.7
Pitching moment	82.5	86.5

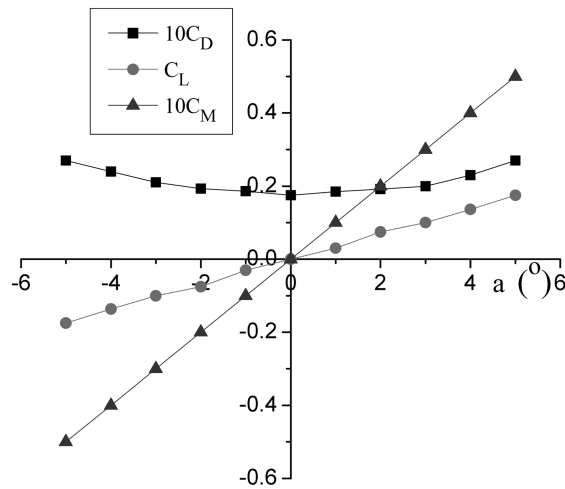


Fig. 8 Steady aerodynamic coefficients of the thin plate section model

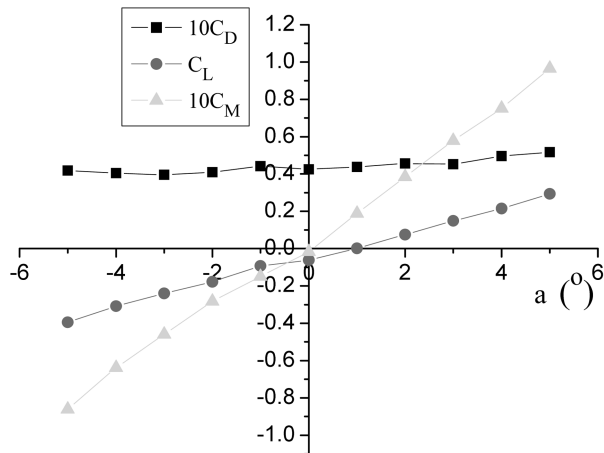


Fig. 9 Steady aerodynamic coefficients of the streamlined section model

test, the vibration frequency of the wings is 1 Hz and unchanged, and the mean wind velocity is changeable and the changing range is 0 m/s ~ 12 m/s.

Fig. 10 and Fig. 11 show the variation of the squared amplitudes and the phases of three identified complex aerodynamic admittance functions versus the reduced frequency for the thin plate section at 0° wind attack angle. The aerodynamic admittance functions χ_{Dw} , χ_{Lu} and χ_{Mu} for the

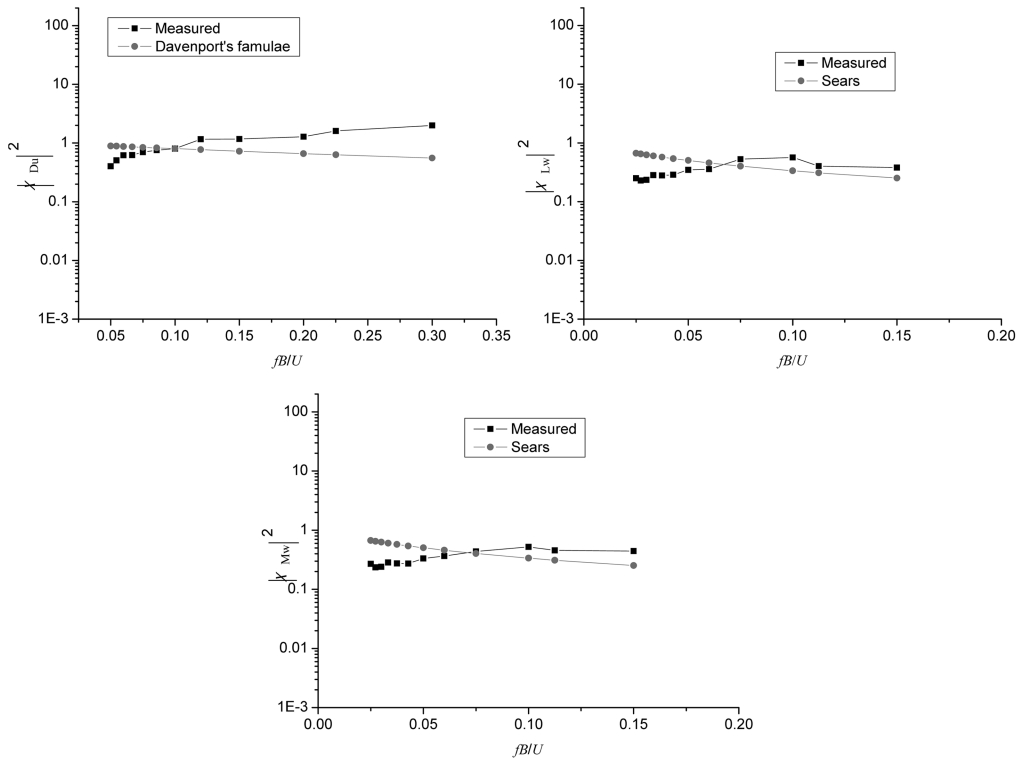


Fig. 10 The squared amplitude of CAAFs for the thin plate section at 0° attack angle

thin plate section are nonexistent because the section is symmetrical about the horizontal axis and its static aerodynamic coefficients C_D' , C_L , C_M are close to zero, as given in Fig. 8. Thus χ_{Dw} , χ_{Lu} and χ_{Mu} for the thin plate section are not shown in Figs. 10 and 11. Similarly, the variation of the squared amplitudes and the phases of the six complex aerodynamic admittance functions versus the reduced frequency for the streamlined section at 0° wind attack angle are shown in Figs. 12 and 13. The measured aerodynamic admittance function χ_{Du} is compared to Davenport's formulae (Davenport 1962). The remaining aerodynamic admittance functions are compared with Sears formulae (Sears 1941).

From Figs. 10 and 12, it is seen that the measured magnitude of aerodynamic admittance functions deviate from those of the Sears function or Davenport's formulae, especially the aerodynamic admittance functions corresponding to the longitudinal component and the admittance functions for drag force. Sears function is the aerodynamic admittance functions of a thin aerofoil associated with the vertical force and in fact caused by the vertical turbulent component. Davenport's formula is the aerodynamic admittance function of drag forces associated with horizontal turbulence component. In addition, the admittance functions corresponding to the longitudinal component are different from those corresponding to the vertical component. Therefore, it is necessary to estimate all the six admittance functions and not just the three equivalent admittance functions. In other words, we cannot simply assume that the admittance functions corresponding to the longitudinal component are equal to those corresponding to the vertical component. Unlike Sears function, some of the identified aerodynamic admittance functions increase with the increase of the reduced frequency. Actually,

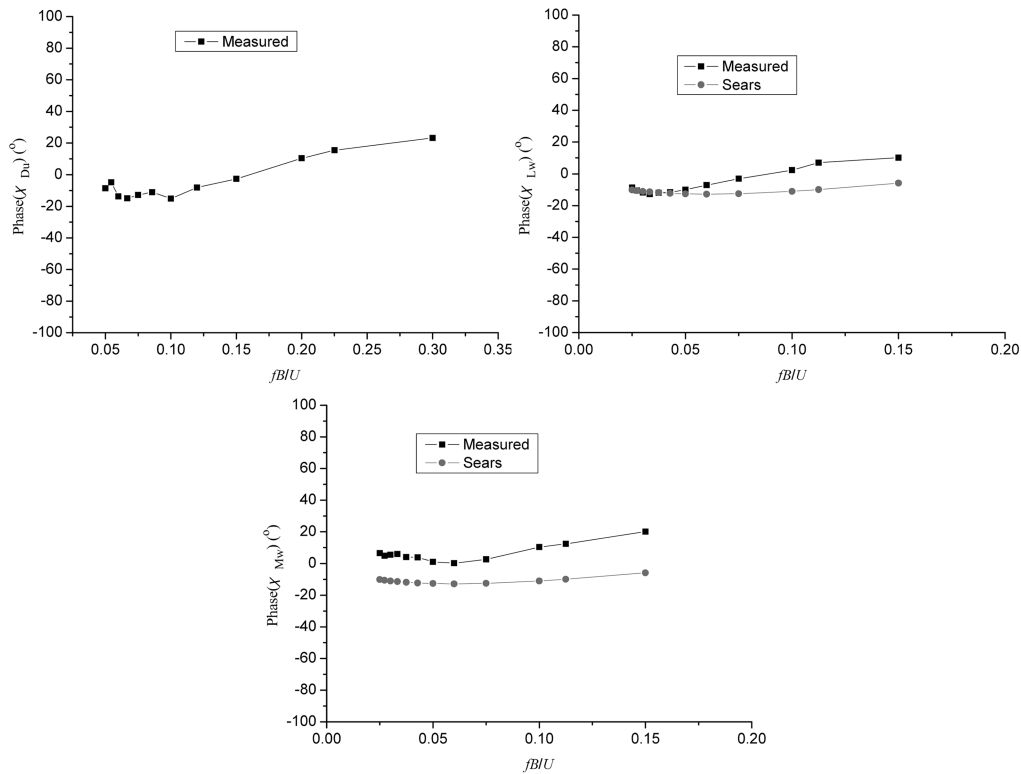


Fig. 11 The phase of CAAFs for the thin plate section at 0° attack angle

similar observations of certain increase trend with the reduced frequency were also made by Scanlan (2000) and Diana, *et al.* (2004) for bridge sections. The value of the aerodynamic admittance functions may also exceed unity for some cases in this study, which was also reported by several other researchers (Larose and Livesey 1997, Larose, *et al.* 1998, Scanlan 2000, Diana, *et al.* 2004). From Figs. 11 and 13, it can be seen that the phases of the estimated admittance functions increase with the increase of the reduced frequency just like Sears functions.

Large vortex shedding will occur and quasi-steady theory may not be applicable in the range of attack angle beyond $\pm 10^\circ$. However, for long-span bridges constructed with mountain area with deep valley, such large attack angle may exist even in strong winds. The admittance function identified in such condition may be explained as ‘equivalent’ admittance functions in conjunction with quasi-steady theory. However, these ‘equivalent’ admittance functions may deviate significantly from the Sears function or Davenport’s formulae. Nevertheless, the characterization of the aerodynamic admittance functions deserves further exploration in the future.

6. Conclusions

A new methodology of estimating the six complex aerodynamic admittance functions is developed by first through theoretical derivations and then by developing experimental techniques. Based on the results of this limited study, the following conclusions are drawn: (1) Drag-force admittance

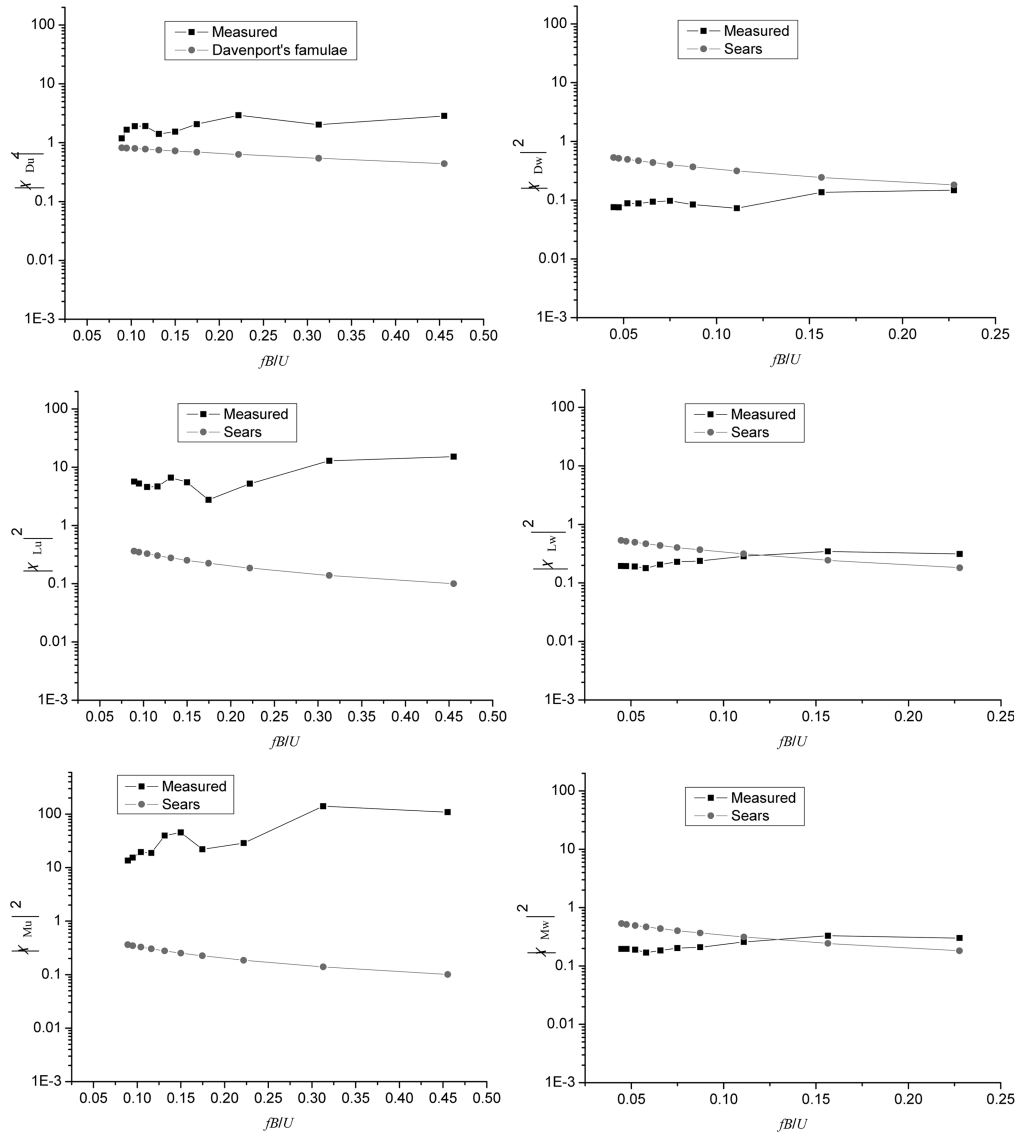


Fig. 12 The squared amplitude of CAAFs for the streamlined section at 0° attack angle

functions and admittance functions corresponding to the longitudinal component deviate significantly from the Sears function. The Sears function can only be employed as an approximation of the lift-force and pitching-moment aerodynamic admittance functions corresponding to the vertical turbulence component when the experimentally determined admittance functions are not available. (2) The admittance functions corresponding to the longitudinal component are different from those corresponding to the vertical component and it is necessary to estimate all the six admittance functions. (3) Some of the identified aerodynamic admittance functions increase with the increase of the reduced frequency. (4) The phases of the estimated admittance functions increase with the increase of the reduced frequency just like Sears functions.

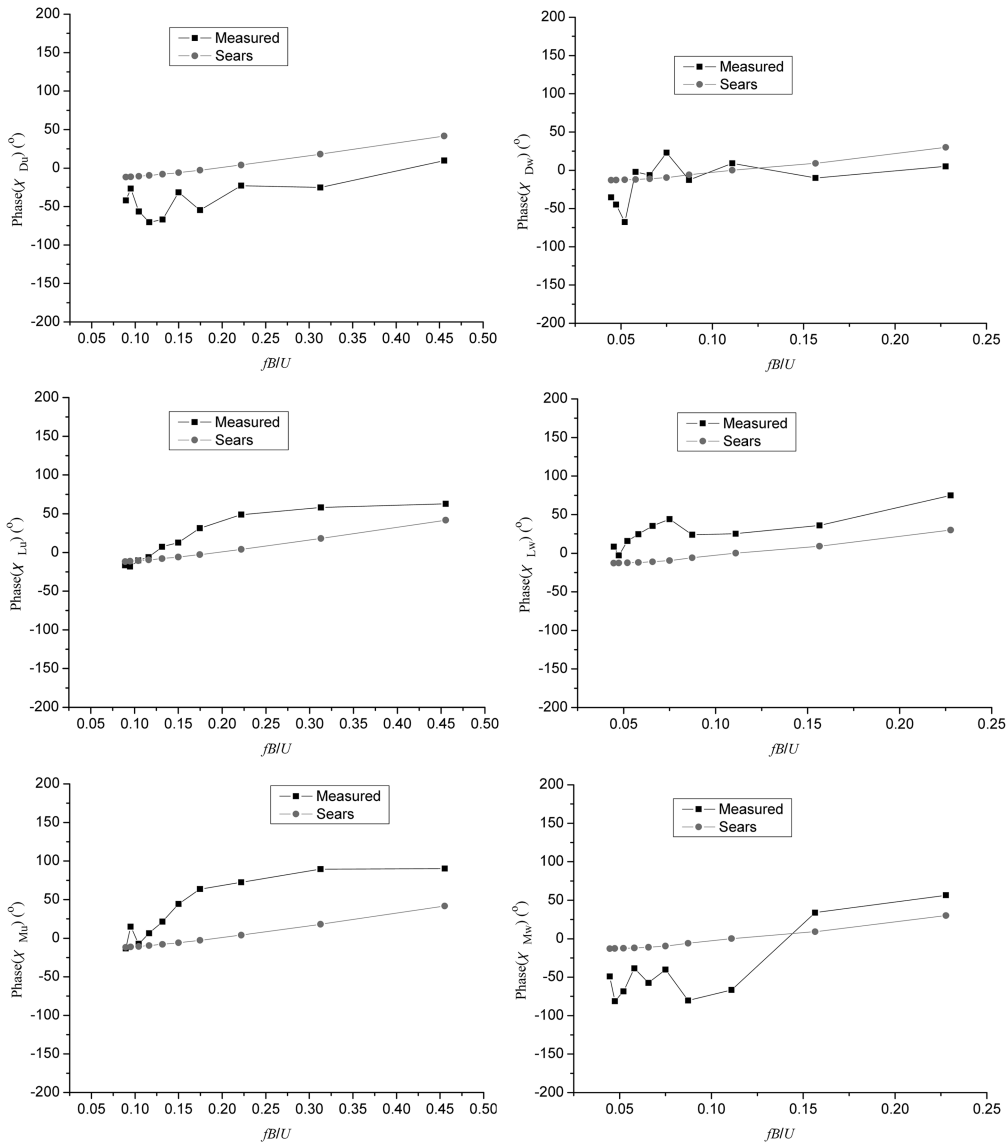


Fig. 13 The phase of CAAFs for the streamline section at 0° attack angle

It is also recommended that more research be performed for the aerodynamic admittance functions to predict the buffeting responses of long-span bridges more accurately.

Acknowledgements

The authors would like to gratefully acknowledge the supports from the National Science Foundation of China (Project Nos. 50478051 and 50738002) and from the Wind Engineering Research Center of Hunan University and the School of Civil Engineering and Architecture of

Changsha University of Science and Technology in China.

References

- Chen, X. and Kareem, A. (2002), "Advances in modeling aerodynamic forces on bridge decks", *J. Eng. Mech.-ASCE*, **128**(11), 1193-1205.
- Davenport, A.G. (1962), "Buffeting of a suspension bridge by storm winds", *J. Struct. Div., ASCE*, **88**(3), 233-268.
- Denoël, V. and Degée, H. (2006), "Influence of the non-linearity of the aerodynamic coefficients on the skewness of the buffeting drag force", *Wind Struct.*, **6**, 457-471.
- Diana, G., Bruni, S., Cigada, A. and Zappa, E. (2002), "Complex aerodynamic admittance function role in buffeting response of a bridge deck", *J. Wind Eng. Ind. Aerod.*, **90**, 2057-2072.
- Diana, G., Resta, F., Zasso, A., Belloli, M. and Rocchi, R. (2004), "Forced motion and free motion aeroelastic tests on a new-concept dynamometric section model of the Messina suspension bridges", *J. Wind Eng. Ind. Aerod.*, **92**, 441-462.
- Han, Y. (2007), *Study on complex aerodynamic admittance functions and refined analysis of buffeting response of bridges*, Ph.D. Thesis, College of Civil Engineering, Hunan University, China. (In Chinese).
- Hatanaka, A. and Tanaka, H. (2002), "New estimation method of aerodynamic admittance function", *J. Wind Eng. Ind. Aerod.*, **90**, 2073-2086.
- Hatanaka, A. and Tanaka, H. (2008), "Aerodynamic admittance functions of rectangular cylinders", *J. Wind Eng. Ind. Aerod.*, **96**, 945-953.
- Jancauskas, E.D. and Melbourne, W.H. (1986), "The aerodynamic admittance of two-dimensional rectangular section cylinders in smooth flow", *J. Wind Eng. Ind. Aerod.*, **23**, 395-408.
- Kawatani, M. and Kim, H. (1992), "Evaluation of aerodynamic admittance for buffeting analysis", *J. Wind Eng. Ind. Aerod.*, **41-44**, 613-624.
- Larose, G.L. and Livesey, F.M. (1997), "Performance of streamlined bridge decks in relation to the aerodynamics of a thin plate", *J. Wind Eng. Ind. Aerod.*, **69-71**, 851-860.
- Larose, G.L. and Mann, J. (1998), "Gust loading on streamlined bridge decks", *J. Fluid. Struct.*, **12**, 511-536.
- Larose, G.L., Tanaka, H., Gimsing, N.J. and Dyrbye, C. (1998), "Direct measurement of buffeting wind forces on bridge decks", *J. Wind Eng. Ind. Aerod.*, **74-76**, 809-818.
- Liepmann, H.W. (1952), "On the application of statistical concepts to the buffeting problem", *J. Aeronaut. Sci.*, **19**, 793-800.
- Mendes, P.A. and Branco, F.A. (2001), "Unbalanced wind buffeting efforts on bridges during double cantilever erection stages", *Wind Struct.*, **4**, 45-62.
- Sears, W.R. (1941), "Some aspects of non-stationary airfoil theory and its practical application", *J. Aeronaut. Sci.*, **8**, 104-108.
- Scanlan, R.H. (1993), "Problematics in formulation of wind-force model for bridge deck", *J. Eng. Mech.-ASCE*, **119**, 1353-1375.
- Scanlan, R.H. and Jones, N.P. (1999), "A form of aerodynamic admittance for use in bridge aeroelastic analysis", *J. Fluid. Struct.*, **13**, 1017-1027.
- Scanlan, R.H. (2000), "Motion-related body-force functions in two-dimensional low-speed flow", *J. Fluid. Struct.*, **14**, 49-63.
- Theodorsen, T. (1935), *General theory of aerodynamic instability and the mechanism of flutter*, NACA Report, No. 496, Langley: U.S. National Advisory Committee for Aeronautics.
- Tubino, F. (2005), "Relationships among aerodynamic admittance functions, flutter derivatives and static coefficients for long-span bridges", *J. Wind Eng. Ind. Aerod.*, **93**, 929-950.
- Zhou, Y. and Kareem, A. (2003), "Aerodynamic admittance functions of tall buildings", *Proc. of the 11th Int. Conf. on Wind Engineering*, June, Lubbock, TX.